Development 130, 2013-2025

doi:10.1242/dev.00376

DEVELOPMENT AND DISEASE

Lack of pendrin expression leads to deafness and expansion of the endolymphatic compartment in inner ears of *Foxi1* null mutant mice

Malin Hulander[1], Amy E. Kiernan[2,*], Sandra Rodrigo Blomqvist[1,*], Peter Carlsson[4], Emma-Johanna Samuelsson[3], Bengt R. Johansson[3], Karen P. Steel[2] and Sven Enerbäck[1,†]

[1]Medical Genetics, Department of Medical Biochemistry, [4]Department of Molecular Biology, [3]The Electron Microscopy Unit, Institute of Anatomy and Cell Biology, Göteborg University, Box 440, SE-405 30 Göteborg, Sweden
[2]MRC Institute of Hearing Research, University Park, Nottingham NG7 2RD, UK

*These authors contributed equally to this work
†Author for correspondence (e-mail: sven.enerback@medgen.gu.se)

Accepted 8 January 2003

SUMMARY

Mice that lack the winged helix/forkhead gene *Foxi1* (also known as *Fkh10*) are deaf and display shaker/waltzer behavior, an indication of disturbed balance. While *Foxi1* is expressed in the entire otic vesicle at E9.5, it becomes gradually restricted to the endolymphatic duct/sac epithelium and at E16.5 *Foxi1* expression in the inner ear is confined to this epithelium. Histological sections, paint-fill experiments and whole-mount hybridizations reveal no abnormality in inner ear development of *Foxi1*$^{-/-}$ mice before E13.5. Between E13.5 and E16.5 the membranous labyrinth of inner ears from null mutants starts to expand as can be seen in histological sections, paint-fill experiments and three-dimensional reconstruction. Postnatally, inner ears of *Foxi1*$^{-/-}$ mice are extremely expanded, and large irregular cavities, compressing the cerebellum and the otherwise normal middle ear, have replaced the delicate compartments of the wild-type inner ear. This phenotype resembles that of the human sensorineural deafness syndrome Pendred syndrome, caused by mutations in the *PDS* gene. In situ hybridization of *Foxi1*$^{-/-}$ endolymphatic duct/sac epithelium shows a complete lack of the transcript encoding the chloride/iodide transporter pendrin. Based on this, we would like to suggest that *Foxi1* is an upstream regulator of pendrin and that the phenotype seen in *Foxi1* null mice is, at least in part, due to defective pendrin-mediated chloride ion resorption in the endolymphatic duct/sac epithelium. We show that this regulation could be mediated by absence of a specific endolymphatic cell type – FORE (forkhead related) cells – expressing *Foxi1*, *Pds*, *Coch* and *Jag1*. Thus, mutations in *FOXI1* could prove to cause a Pendred syndrome-like human deafness.

Key words: Forkhead, Foxi1, Pendrin, Deafness, Inner ear, Mouse

INTRODUCTION

Hearing loss is a common form of sensory impairment, and several millions of individuals are affected world wide (Wilson, 1985). Around one in a thousand children are born with a significant permanent hearing impairment, and this proportion increases with age until 60% of the population over 70 show an impairment of 25dB or greater (Fortnum et al., 2001; Davis, 1995). In most instances, the inner ear is the primary site of the dysfunction. The inner ear is also one of the most complex organs that has evolved in vertebrates. Originating from the otic placode, a thickening of the surface ectoderm of the head, the inner ear develops gradually through invagination and formation of an otic vesicle by day E9.5 in mice. The sensory hair cells responsible for hearing are located within the organ of Corti in the cochlea. Their function is to convert the energy transmitted by sound waves into neural impulses (Corey and Hudspeth, 1983; Howard and Hudspeth, 1988) and to act as a selective amplifier (Zheng et al., 2000). The vestibular sensory organs, the cristae of the semicircular ducts and maculae of the utricle and saccule, detect angular and linear acceleration, respectively. One crucial aspect of inner ear architecture is the presence of two isolated chambers containing endolymph (high K^+, low Na^+) and perilymph (low K^+, high Na^+). During sound stimulation, deflection of a specialised array of finger-like projections (stereocilia) from the top of each hair cell opens transduction channels. This allows potassium ions to leave the potassium rich endolymph with its positive endocochlear potential, and enter the hair cell with its negative intracellular resting potential. This flood of potassium depolarises the hair cell and triggers synaptic activity leading to action potentials in the cochlear neurons. The endocochlear potential is maintained by active pumping of potassium by stria vascularis cells fed by rapid recycling of potassium ions within the cochlear duct (Steel, 1999). The endolymphatic duct and sac are structures thought to serve as sites for resorption of

endolymph as well as an expansion chamber that can compensate for sudden changes in endolymph volume (Barbara et al., 1988a; Everett et al., 1999). Several ion channel and pump proteins, that assist in maintaining proper ionic composition of the endolymph, are expressed at various specific locations throughout the inner ear epithelium, e.g. the dark cells adjacent to the maculae, stria vascularis of the cochlea and the endolymphatic duct/sac epithelium. Appropriate ionic composition of the endolymph is a prerequisite for normal inner ear function. Mutations in genes encoding such ion channels and pumps have been shown to cause deafness e.g. *KCNQ4* (Kubisch et al., 1999), *KCNQ1* (Neyroud et al., 1997), *KCNE1* (Vetter et al., 1996), *Slc12a2* (Delpire et al., 1999; Dixon et al., 1999), *ATP6B1* (Karet et al., 1999) and *PDS* (Li et al., 1998). Deafness genes may also influence ionic balance of the endolymph by affecting the integrity of the surrounding endolymphatic epithelium or other cell types involved in recycling and/or production of endolymph, e.g. connexin 26, 30 and 31 (Steel and Bussoli, 1999) and *COCH* [encodes a secreted protein, thought to be involved in some cases of Ménière's disease (Fransen et al., 1999)]. *Slc12a2* encodes a Na-K-Cl cotransporter expressed in the marginal cells of stria vascularis, the major site of endolymph production, and mutations in this gene result in failure to produce endolymph. This has been demonstrated by gene targeting experiments as well as by identification of mutations in this gene in the mouse mutant *shaker-with-syndactylism* [*sy* (Delpire et al., 1999; Dixon et al., 1999)]. In both instances, there are clear signs of decreased endolymph production, such as extensive collapse of Reissner's membrane and vestibular walls together with thinning of the semicircular canals. The *Kcne1* mouse mutant shows a similar collapse of endolymphatic compartments (Vetter et al., 1996). Even though several inner ear conditions such as Ménière's disease and Pendred syndrome have been linked to increased volume and/or pressure of the endolymph (Everett et al., 1999), no good model for the pathogenic mechanisms underlying these conditions have been presented.

Here we describe the *Foxi1*$^{-/-}$ (*Fkh10*) mutant in which the endolymphatic compartment is severely dilated. We show that these mice are deaf and lack an endocochlear potential, indicating a primary defect in fluid homeostasis in the inner ear. This is associated with an expansion of the endolymph compartment followed by rupture of the endolymphatic epithelium. Based on morphological, physiological and genetic analysis we propose a molecular mechanism by which the endolymphatic inner ear fluid is allowed to accumulate to abnormal levels.

MATERIALS AND METHODS

Mice

Foxi1 mutant mice (Hulander et al., 1998) and wild-type littermates of CD-1 and Bl6 origin were obtained from heterozygous crosses. Genotypes were determined from tail biopsies using PCR. The forward primer 5′-CCT TCG ACC TCC CAG CGC CTT-3′ and the two reverse primers 5′-GGG CAG TAG CTG CCT CTG CAT-3′ and 5′-GGG CCA GCT CAT TCC TCC ACT-3′ yielded 290 bp wild-type and 320 bp mutated allele products in a 30-cycle reaction (95°C for 30 seconds 65°C for 30 seconds 72°C for 15 seconds).

Histology and hybridization

The morning that vaginal plugs were detected was designated embryonic day 0.5 (E0.5). Tails from embryos were collected for genotyping using PCR as described above. Embryos were fixed overnight in PBS with 4% paraformaldehyde at 4°C. For histological examination, embryos were dehydrated and embedded in paraffin wax and 6 μm sections were cut. Tissue sections were stained with Haematoxylin and Eosin. In situ hybridization on whole-mount mouse embryos (Rosen and Beddington, 1993) and in situ hybridization of cryosections (Bostrom et al., 1996) were performed with digoxigenin-labeled antisense cRNA probes. No signals were observed when control sense probes were used. We used plasmids to generate probes for: *Pds* (Everett et al., 1999), *Pax2* (Torres et al., 1996), *ErbB3* (Britsch et al., 1998), *Eya1* (Xu et al., 1999), *Hmx3* (Wang et al., 1998), *Jag1* (Morrison et al., 1999), *Otx1* (Acampora et al., 1996) and *Coch* (Robertson et al., 1997). For histology and in situ hybridization experiments inner ears from at least seven mice of each genotype (*Foxi1*$^{+/+}$, *Foxi1*$^{+/-}$ and *Foxi1*$^{-/-}$) of CD-1 background and three of each genotype of Bl6 background were analyzed.

Immunohistochemistry

For BrdU labeling, pregnant female mice were injected intraperitoneally with BrdU (1 ml of 10 mM BrdU per 100 g body weight; Roche). Injected mice were sacrificed 2 hours later and processed for immunohistochemistry, according to protocols supplied by the manufacture. Kits (Roche) were used to identify apoptotic cells by the TUNEL assay according to the manufacturer's instructions. For immunohistochemistry, BrdU labeling experiments and TUNEL assay inner ears from at least four mice of each genotype (*Foxi1*$^{+/+}$, *Foxi1*$^{+/-}$ and *Foxi1*$^{-/-}$) of CD-1 background were analyzed.

Paint-fill

Paint-filling of inner ears (E11.5: *Foxi1*$^{+/+}$; n=5, *Foxi1*$^{+/-}$; n=3, *Foxi1*$^{-/-}$; n=3, E12.5: *Foxi1*$^{+/+}$; n=3, *Foxi1*$^{+/-}$; n=8, *Foxi1*$^{-/-}$; n=3, E16.5: *Foxi1*$^{+/+}$; n=6, *Foxi1*$^{+/-}$; n=11, *Foxi1*$^{-/-}$; n=5) was performed in a similar way to that described for chicken and mouse embryos (Martin and Swanson, 1993). Briefly, mice (E11.5-E16.5) were decapitated and fixed in Bodian's fixative (75% ethanol, 5% formalin, 5% glacial acetic acid) overnight and dehydrated twice in each of the following solutions: 75%, 95%, 100% ethanol (minimum 2 hours for each wash). Heads were bisected and cleared overnight in methyl salicylate. The endolymphatic compartment of the inner ear was injected via either the common crus and/or cochlea using a pulled glass capillary pipette (20-40 μm diameter) filled with 1% gloss paint in methyl salicylate. The ears were then dissected free of the skull and photographed in methyl salicylate. Temporal bone biopsies were cleared in methyl salicylate for analysis of otoconial crystals.

Three-dimensional reconstruction

Three-dimensional reconstructions from inner ears were made using approximately 300 serial sections (6 μm) from an entire inner ear. The inner lumen of the ear was traced and sensory areas, identified by the typical pseudostratified appearance of the epithelium, were outlined in different colors. Areas of interest from each section were traced, aligned and reconstructed into three-dimensional images essentially as has been described earlier (Wu and Oh, 1996). For data processing we used the computer software Spyglass Slicer/T3D (Research System, http://www.researchsystems.com/noesys). Four skulls of each genotype (*Foxi1*$^{+/+}$, *Foxi1*$^{+/-}$ and *Foxi1*$^{-/-}$) of CD-1 background were sectioned and all four in each group had identical phenotypes. Two of each genotype were used for three-dimensional reconstruction.

Skeleton staining

The embryos were fixed in 95% ethanol and stained with Alizarin Red to reveal bone and Alcian Blue to reveal cartilage (McLeod, 1980). They were subsequently cleared by trypsin digestion and KOH treatment, and stored in glycerol.

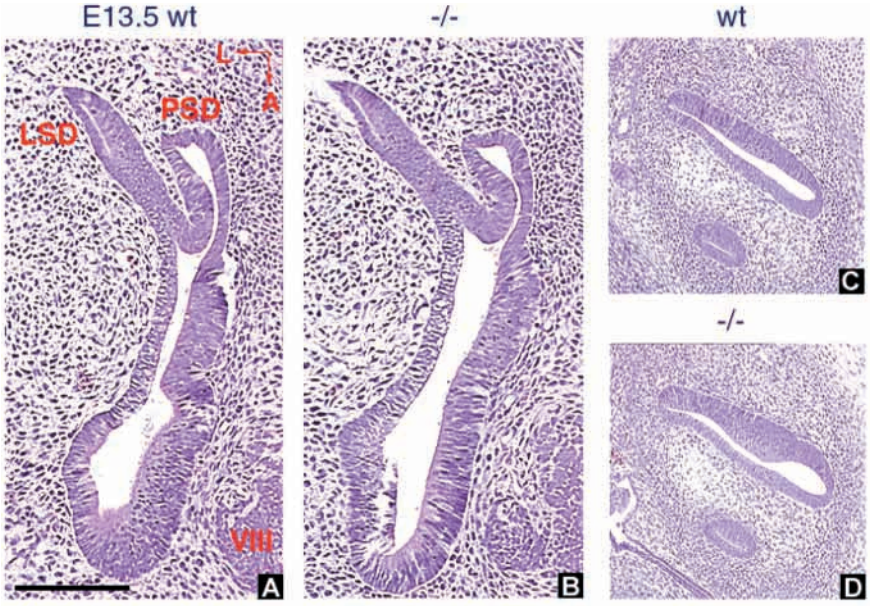

Fig. 1. Inner ear histology of *Foxi1*$^{+/+}$ and *Foxi1*$^{-/-}$ mice at E13.5 (A-D). Lateral (L) and anterior (A) orientations as marked in A. At E13.5 (A,B), normal vestibulocochlear ganglion (VIII), lateral (LSD) and posterior (PSD) semicircular ducts are formed in both *Foxi1*$^{+/+}$ and *Foxi1*$^{-/-}$ animals. There is also a developing cochlea of normal appearance (C,D). Scale bar: 100 μm.

Scanning electron microscopy

Heads of E14.5 embryos were fixed immediately after decapitation in a mixture of 2% paraformaldehyde, 2.5% glutaraldehyde, 0.1% sodium azide in 0.05 M sodium cacodylate buffer, pH 7.2. The heads were embedded in 7% agar and serial sections were obtained with an oscillating tissue slicer (Leica VT 1000S; section thickness set at 200 μm, horizontal orientation). The slices were examined in a tissue preparation microscope to identify levels with opened endolymphatic structures. Selected sections were further treated with a repeated sequence of 1% osmium tetroxide and a saturated thiocarbohydrazide solution (OTOTO method), followed by dehydration in ethanol and infiltration in hexamethyldisilazane (HMDS). The specimens were dried by evaporation of the HMDS in a fume hood and were flat mounted on aluminum stubs. They were examined in a Zeiss 982 Gemini field emission scanning electron microscope without prior thin film metal coating.

Electrophysiology

Mice (n=5 controls (2 *Foxi1*$^{+/+}$, 3 *Foxi1*$^{+/-}$); 5 *Foxi1*$^{-/-}$, aged 29-30 days; and n=6 *Foxi1*$^{+/+}$; 6 *Foxi1*$^{+/-}$; 5 *Foxi1*$^{-/-}$ aged 67-68 days) were anaesthetized with urethane, the middle ear was opened, and a recording electrode was placed on the round window of the cochlea. A closed sound system in the external ear canal was used to deliver calibrated tonebursts (15 mseconds duration, 1 mseconds rise/fall time, 100 mseconds interstimulus interval, average 200 repetitions). Thresholds for detection of a cochlear nerve compound action potential (CAP) response were obtained using 2-3 dB steps. The endocochlear potential (EP) was measured in the same animals as well as in additional ones (*Foxi1*$^{+/+}$, n=12; *Foxi1*$^{+/-}$, n=15; *Foxi1*$^{-/-}$, n=14) using a micropipette electrode inserted into the basal turn scala media through the lateral cochlear wall (Steel and Smith, 1992).

RESULTS

In earlier work, we described the otic vesicle-restricted expression pattern of *Foxi1* at E9.5 and the cystic dilatation of the inner ears at E18.5 in mice that lack *Foxi1* (Hulander et al., 1998). As a likely consequence of this dilatation, such mice display hearing and balance problems (Hulander et al., 1998). Here we present a more detailed analysis of the morphological, physiological and genetic consequences for inner ear development that proceeds without the participation of the winged helix gene *Foxi1*.

Morphological analysis of inner ear development from E11.5 to E13.5

From earlier experiments, it was known that otic vesicle formation at E9.5 is unaffected in *Foxi1* null mutants (Hulander et al., 1998). To investigate the morphology in wild type and *Foxi1*-deficient mice during later stages of inner ear development, we compared the histology using sections from E11.5 (not shown), E12.5 (not shown) and E13.5 (Fig. 1). At E11.5 formation of the endolymphatic appendage, the cochlear anlagen and the vertical plate of the vestibular system (future anterior and posterior semicircular ducts) is seemingly unaffected in mice that lack *Foxi1* (not shown). From E12.5-13.5, we find a normal cochlea as well as normal semicircular ducts in both wild-type and *Foxi1*$^{-/-}$ mice (not shown). At E11.5, the combined facial and vestibulo-cochlear ganglion (cranial nerve ganglion VII and VIII) is present and at E12.5 to E13.5 the vestibulo-cochlear ganglion (VIII) has formed in both wild type and null mutants. To assess the general morphology of the membranous labyrinth we used a paint-fill method in which a thin needle was inserted into the most cranial part of the common crus, formed by the anterior and posterior semicircular ducts (Martin and Swanson, 1993). Subsequently white gloss paint was injected to visualize the endolymphatic compartment. The future endolymphatic and semicircular ducts as well as saccule and cochlea showed no signs of abnormality at E11.5 and E12.5 (Fig. 2). As illustrated (Figs 1, 2) no apparent difference in morphogenesis can be seen at early stages of inner ear development.

Expression of inner ear marker genes at E11.5

At E11.5 *Foxi1* expression is restricted to the otocyst with most of the staining in structures that will give rise to the endolymphatic duct and sac (Fig. 3). Based on earlier findings (Hulander et al., 1998) and data presented in Fig. 3 it is clear that *Foxi1* expression is restricted to the otic vesicle from E9.5 to E11.5. To study the possibility that *Foxi1*$^{-/-}$ embryos could be affected in their capacity to express other genes of importance for inner ear development, without causing any detectable morphological aberration (Figs 1, 2) at early developmental stages (E11.5-E13.5) we performed whole-mount hybridization on E11.5 wild-type and *Foxi1*$^{-/-}$ embryos using cRNA probes encoding five inner ear marker genes. (i) *ErbB3*, a marker for neural crest-derived cell populations, i.e. presumptive stria vascularis cells (Britsch et al., 1998; Lemke,

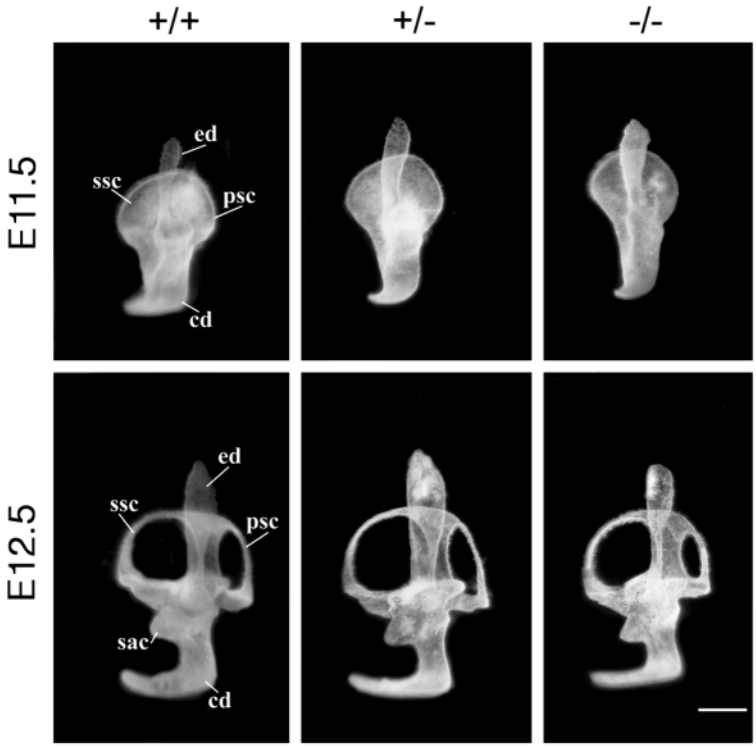

Fig. 2. Paint-filled inner ears of E11.5 and E12.5 embryos. No major differences can be demonstrated when the three (*Foxi1*$^{+/+}$, *Foxi1*$^{+/-}$ and *Foxi1*$^{-/-}$) genotypes are compared. ssc (superior semicircular canal), psc (posterior semicircular canal), cd (cochlear duct) ed (endolympahtic duct) and sac (saccule) are indicated. Scale bar: 250 μm.

1996). (ii) *Otx1*, necessary for proper induction of the lateral canal as well as utriculosaccular and cochleosaccular ducts (Acampora et al., 1996; Morsli et al., 1999). (iii) *Eya1*, crucial for inductive signaling events during early otic vesicle maturation (Sahly et al., 1999; Xu et al., 1999). (iv) *Pax2*, expressed in regions of the otocyst that will give rise to cochlea and saccule (Favor et al., 1996; Hutson et al., 1999; Torres et al., 1996) as well as in prospective endolymphatic epithelium (Lawoko-Kerali et al., 2002). Mice lacking *Pax2* are void of cochlea (Torres et al., 1996; Favor et al., 1996). (v) *Hmx3* (also known as *Nkx5-1*) is required for proper formation of the sensory organs of the vestibulum (Hadrys et al., 1998; Wang et al., 1998). These five marker genes showed identical staining pattern in *Foxi1*$^{-/-}$ and wild-type litter mates (not shown).

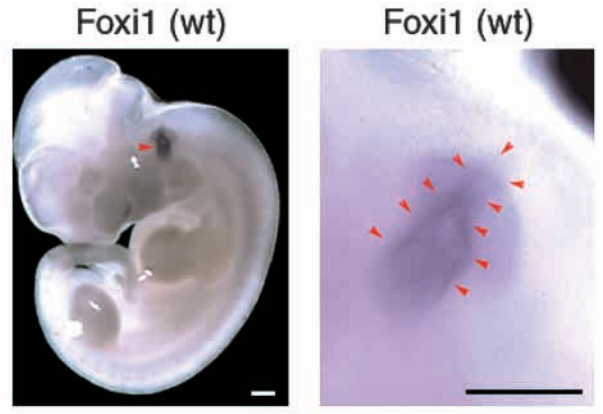

Fig. 3. Whole-mount in situ hybridization of E11.5 wild-type embryo. *Foxi1* has an otic vesicle-specific expression pattern (left panel, red arrowhead). At higher magnification (right panel), the contours of the future endolymphatic duct can be seen (arrowheads). Scale bars: 100 μm.

Inner ears of *Foxi1* null mutants are expanded at E16.5

Histological sections comparing inner ear morphology in wild-type and *Foxi1* mutant embryos reveal an expansion of several inner ear structures at E16.5 (Fig. 4A-D). The entire inner ear seems to be expanded including the posterior semicircular duct, common crus (not shown), ampullae (not shown) and the cochlea. However, the most prominent enlargement is seen in the endolymphatic duct/sac (Fig. 4A,B). The apical turn of the cochlea has been replaced by an apical cyst, the basal turn is also enlarged (Fig. 4C,D). In paint-fill experiments using inner ears of embryos from E16.5 the picture is quite different from that at E11.5 and E12.5. There is a prominent expansion of the entire membranous labyrinth. The endolymphatic duct and sac together with the saccule, utricle, ampullae and cochlea are all severely enlarged whereas the semicircular ducts seem to be less affected (Fig. 5). A three-dimensional image was reconstructed using approximately 300 serial sections representing an entire inner ear at E16.5 (Fig. 6). This experiment allowed us to visualize the membranous labyrinth and at the same time mark the sensory areas of the inner ear.

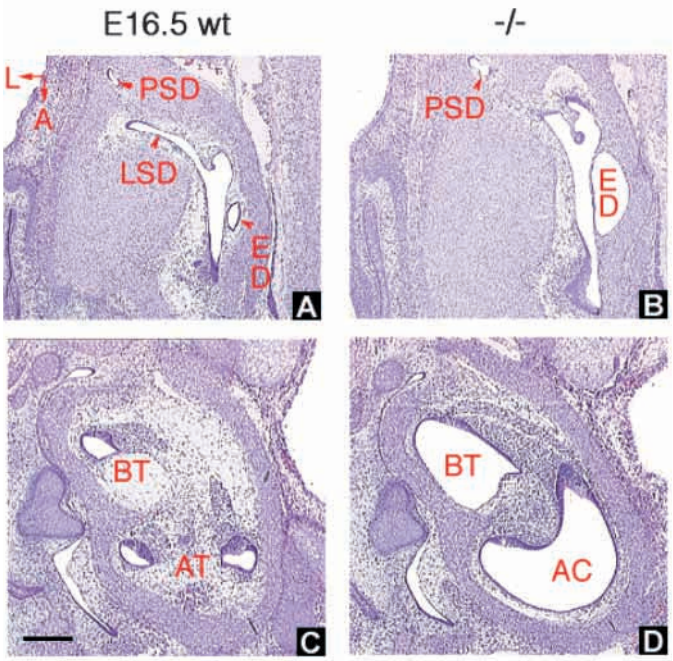

Fig. 4. Histology of inner ears from *Foxi1*$^{+/+}$ and *Foxi1*$^{-/-}$ embryos at E16.5. (A,B) The lateral (LSD) and posterior (PSD) semicircular ducts as well as the endolymphatic duct (ED) are expanded in the mutant ear. (C,D) In the cochlea of *Foxi1*$^{-/-}$ ear the basal turn (BT) is larger and the apical turn (AT) has formed an apical cyst (AC). Scale bar: 200 μm for A,B; 100 μm for C,D .

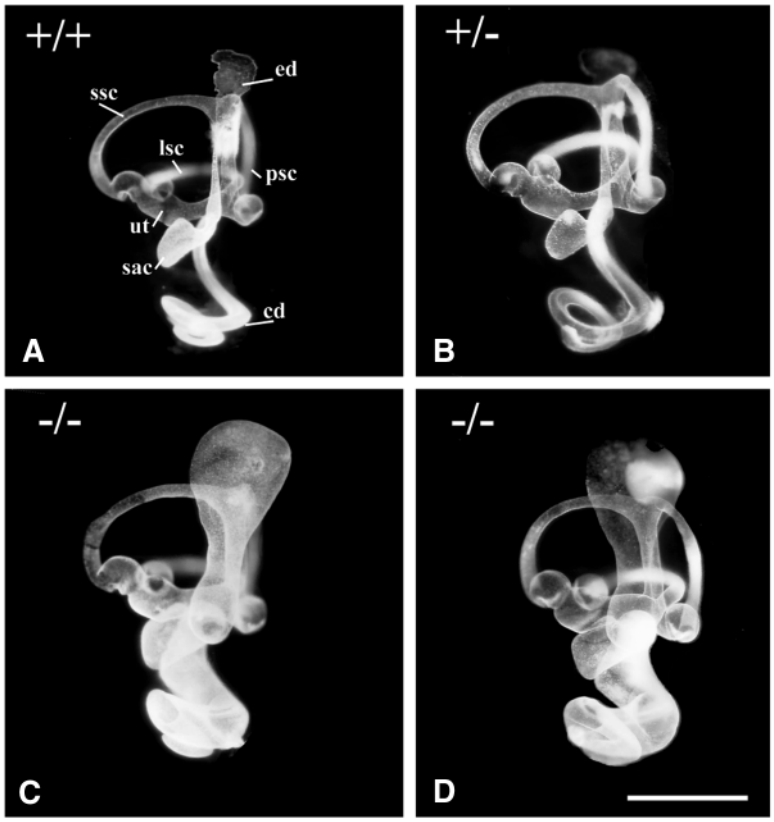

Fig. 5. Paint-filled inner ears from E16.5 mice. Superior (ssc), lateral (lsc), posterior (psc) semicircular canals, endolymphatic duct (ed), utricle (ut), saccule (sac) and cochlear duct (cd) are all clearly expanded in *Foxi1*$^{-/-}$ embryos (C,D) whereas *Foxi1*$^{+/+}$ (A) and *Foxi1*$^{+/-}$ (B) inner ears appear normal. Scale bar: 1 mm.

This analysis corroborates the results from histological examination (Fig. 4) and paint-fill experiments (Fig. 5). It also demonstrates that the sensory patches in both the vestibulum and the cochlea are located normally. From these data it is clear that while inner ear formation proceeds without any major aberration up to E13.5, an expansion of the entire compartment is evident at E16.5. Measurements of the diameter of the endolymphatic duct at corresponding anatomical sites reveal an increase in diameter of mutant ducts, expressed as arbitrary units [42.3±4.7 (s.d., n=3)], compared with wild-type ducts [11.0±1.0 (s.d., n=3), P<0.01]. The ratio of mutant over wild-type diameter is 3.8, this ratio predicts an increase in volume by a factor of approximately 55 (3.8^3=54.9), assuming an equal and proportional increase in all three dimensions.

At P12 inner ears of Foxi1$^{-/-}$ mice are severely affected by progressive dilation

To investigate whether the expansion noted at E16.5 was transient or progressive in nature, a histological examination of decalcified skulls from postnatal day 12 (P12) mice was performed. From this analysis it is clear that the expansion is progressive and that the entire inner ear is replaced by large irregular cavities (Fig. 7A-D). The saccule and utricle have expanded and formed a large cavity that is continuous with the endolymphatic duct and sac (Fig. 7A,D). The basal turn of the cochlea has expanded and ruptured into a common cavity, and this is also true for the apical turn that forms an apical cyst in the mutant cochlea (Fig. 7B,D). Since the modiolus is missing in the cochlea of *Foxi1* mutant mice (Fig. 7D) the phenotype fulfills the criterion for a Mondini malformation of the cochlea as described by Carlo Mondini in 1791 (Mondini, 1791). The extreme expansion of the inner ear also seems to compress the cerebellum raising the intriguing possibility that the balance problems seen in *Foxi1*$^{-/-}$ mice (Hulander et al., 1998) could be derived to some extent from a direct compression of the cerebellum. The temporal bone, in which the entire inner ear resides, is thinner adjacent to the inner ear (Fig. 7C). A thinning of the endolymphatic epithelium in both the endolymphatic duct (Fig. 4B) and the cochlea (Fig. 4D) is evident already at E16.5. The cystic appearance of the cochlea (Fig. 7D; no sign of perilymphatic compartment) as well as the disrupted compartmentalization of the vestibular portion of the inner ear at P12 (Fig. 7C) strongly suggest that the peri- and endolymphatic compartments of the inner ear in *Foxi1* mutants, at P12, have been replaced by a common irregular cavity.

The otoconia of the utricle and saccule were investigated in methyl salicylate-cleared temporal bone specimens from mutants and controls (Fig. 8). Here we found a complete absence of normal-looking otoconia in the mutant mice whereas *Foxi1*$^{+/-}$ mice displayed the normal white otoconial appearance. This might reflect an inability to form proper crystals in the mutant mice. The expansion and altered ability to form otoconia could reflect an altered ionic composition of the endolymph.

Another possible mechanism explaining the expanded inner ear phenotype would be an altered rate of apoptosis and/or cell proliferation. In a TUNEL labeling experiment, performed on sections from E16.5, only one minor difference in labeled cell populations were detected (Fig. 9). A small mesenchymal cell population adjacent to the lateral border of the endolymphatic duct showed increased TUNEL labeling (Fig. 9). A BrdU labeling experiment was also performed at E16.5 and no difference in the number of labeled cells could be detected (not shown). These results suggest that only minor differences exist in the rate of apoptosis and cell proliferation at E16.5, a time point at which the inner ear has initiated its expansion. Yet another explanation for the inner ear phenotype observed in *Foxi1* mutants could be a defect in epithelial-mesenchymal interactions during condensation of the periotic mesenchyme. To address this, bone and cartilage staining was performed on E18.5 embryos. Normal integration of the inner ear into the temporal bone anlagen was observed in wild-type and *Foxi1*$^{+/-}$ embryos whereas null mutants displayed an abnormal integration associated with ectopic cartilage and/or bone formation (Fig. 10). In conclusion, these experiments demonstrate an extremely expanded inner ear with lack of a proper crystallization of the otoconia, which points toward an altered ionic composition of the endolymph as the underlying cause of this phenotype. According to this hypothesis, the increased amount of

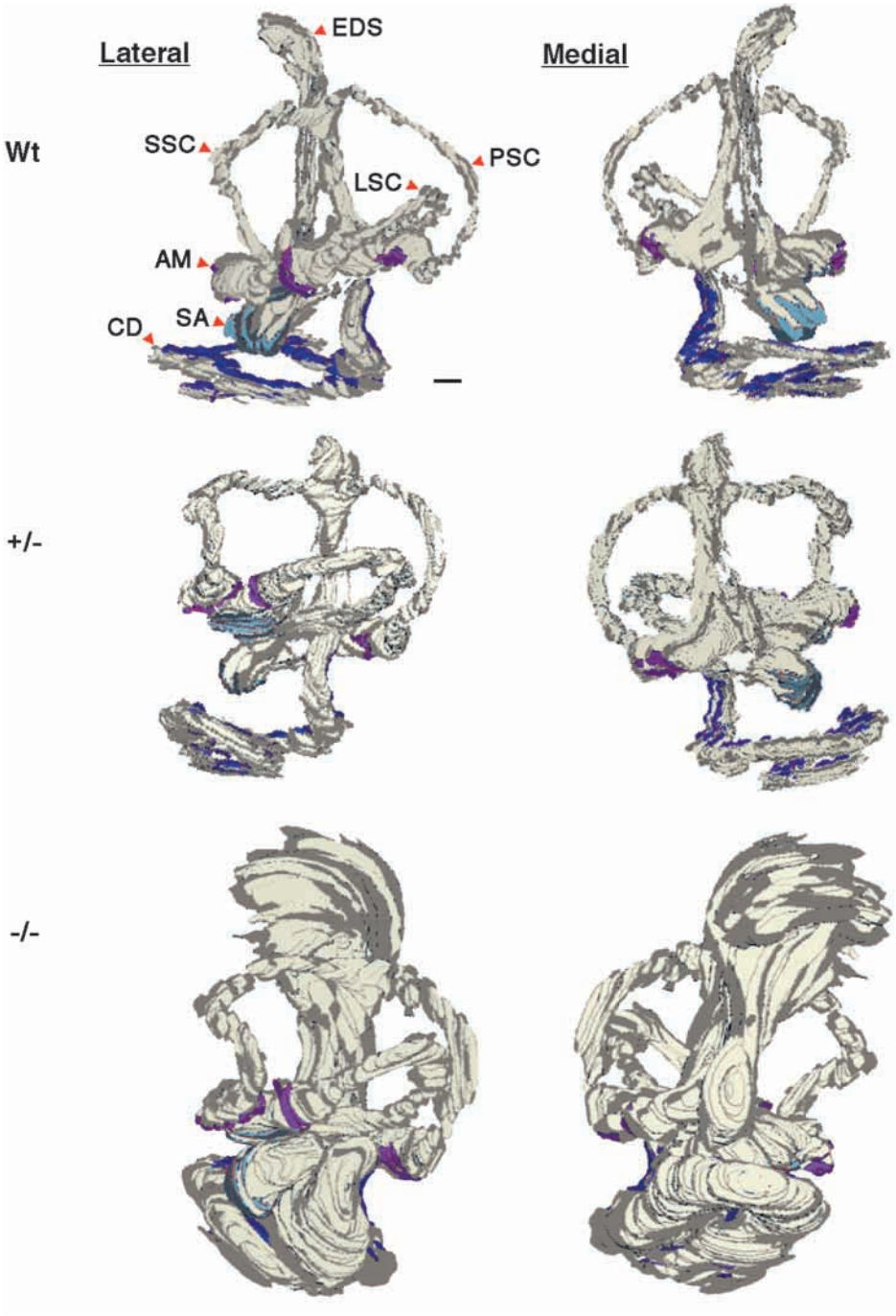

Fig. 6. Three dimensional reconstruction of E16.5 inner ears using 6 μm tissue sections. Lateral and medial views are shown. am, ampulla; other abbreviations as in Figs 1-4. Sensory patches are marked in the cochlea (dark blue), saccule and utricle (light blue), and in the ampullae (purple). In spite of the enormous expansion in the *Foxi1*$^{-/-}$ inner ear, the sensory patches can be identified at approximately the correct locations. In the tissue sections used in this experiment the sensory areas appear normal in all three genotypes (not shown). Scale bar: 100 μm.

apoptotic cells adjacent to the endolymphatic duct (Fig. 9) as well as the abnormal integration of the inner ear in the temporal bone (Fig. 10) probably should be regarded as phenomena secondary to the expansion.

Foxi1 mutants are deaf and lack an endocochlear potential

Previously, we have shown that *Foxi1* mutant mice do not respond in a Preyer reflex test, which is a crude single frequency hearing test, indicating profound hearing impairment (Hulander et al., 1998). In order to test the hearing of these mice with better accuracy we performed round window recordings. This enabled us to record compound action potentials (CAP) as the result of sound stimulation of various intensities and frequencies. As shown in Fig. 11A, no thresholds could be established for any of the frequencies tested in *Foxi1*$^{-/-}$ mice, a finding compatible with complete hearing loss. The thresholds measured for *Foxi1*$^{+/+}$ and *Foxi1*$^{+/-}$ mice were not significantly different from each other but did show relatively high thresholds compared with other strains of mouse, especially at high frequencies (Fig. 11A) (Shone et al., 1991). Endocochlear potentials (EP) were also measured and as can be seen in Fig. 11B they were normal (approximately +115 mV) in wild-type and heterozygotes whereas null mutants have an EP of about 0 mV.

Foxi1 regulates expression of the Pds, Coch and Jag1 genes in endolymphatic duct/sac epithelium

With these results at hand, we sought a molecular explanation for the morphological and physiological findings observed in *Foxi1*$^{-/-}$ mice. Pendred syndrome (PDS) is a human congenital sensorineural deafness syndrome caused by mutations in the *PDS* gene, characterized by, among other things, a widened vestibular aqueduct, Mondini malformation of the cochlea as well as an enlarged endolymphatic duct and sac (Everett et al., 1997; Johnsen et al., 1986; Phelps et al., 1998). Since the phenotype described for Pendred syndrome and that observed in *Foxi1*$^{-/-}$ mice show clear similarities, we used a mouse *Pds* cRNA probe for hybridization experiments on inner ear tissue sections from wild type and null mutants (Fig. 12A-C). The wild-type expression patterns of the *Pds* and *Foxi1* genes are very similar, being scattered within the endolymphatic duct/sac epithelium (Fig. 12A). At this developmental stage (E16.5), *Foxi1* expression is restricted to the endolymphatic duct/sac epithelium while the *Pds* gene is expressed in the external sulcus of the cochlea as well as adjacent to the maculae of the saccule and utricle (Fig. 12C).

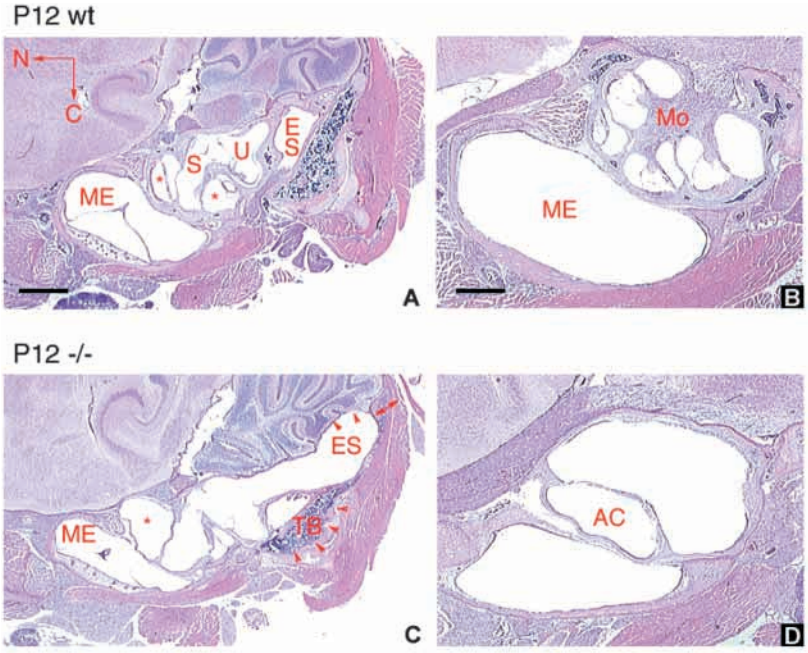

Fig. 7. Histology of inner ears of P12 *Foxi1*$^{+/+}$ and *Foxi1*$^{-/-}$ mice. Nasal (N) and caudal (C) orientations as marked in A. In *Foxi1*$^{-/-}$ mice the entire inner ear is enlarged with large irregular cavities in place of the delicate inner ear structures of the wild-type ear. S, saccule; U, utricle; ME, middle ear; asterisks mark the basal turn of the cochlea in A. (C) In the mutant the endolymphatic sac (ES) seems to compress the cerebellum and the posterior part of the ES (arrowheads) is expanded considerably in the posterior/dorsal direction (double headed arrow) compared with the wild type (A). The temporal bone (TB, arrowheads) is also clearly reduced. (B,D) The normal cochlea with its modiolus (Mo, in B) is absent in the mutant (D) and in its place is an enlarged cavity with an apical cyst (AC). Scale bars: in A, 100 μm for A,C; in B, 100 μm for B,D.

In *Foxi1*$^{-/-}$ mutants there is a complete lack of *Pds* gene expression in the endolympahtic duct/sac epithelium (Fig. 12B). It is interesting to note that only in locations where expression of *Foxi1* and *Pds* overlap can we demonstrate a lack of *Pds* gene expression, i.e. the endolymphatic duct/sac epithelium (Fig. 12B). In spite of altered morphology of the cochlea and utricle in *Foxi1*$^{-/-}$ mice, *Pds* gene expression can be demonstrated at these locations (Fig. 12C). The *COCH* gene is thought to encode a secreted protein with similarities to extracellular matrix proteins (Robertson et al., 1997). It is expressed at high levels in the cochlear and vestibular organs, in the stroma beneath the epithelium as well as in spindle shaped cells along the pathway of auditory nerve fibers (Robertson et al., 1998). *Coch* is expressed in a scattered pattern in the endolymphatic duct/sac epithelium of wild-type embryos whereas this expression is absent in *Foxi1*$^{-/-}$ mice (Fig. 12D). To our knowledge this is the first time that *Coch* expression has been identified in endolymphatic duct/sac epithelium. In other locations such as the cochlea and saccule *Coch* expression is unaffected in *Foxi1* null mutants (Fig. 12E,F). The same is true for expression of the Notch ligand *Jag1* [also known as *Serrate1* (Morrison et al., 1999)], in that *Jag1* is expressed in a punctuate pattern in the endolymphatic duct/sac epithelium and the expression at this location is absent in *Foxi1*$^{-/-}$ animals (Fig. 12G). *Jag1* expression, at other locations of the inner ear, such as the prospective sensory patches at E13-17 and later in supporting cells, is unaffected in the *Foxi1* null mutant (Fig. 12G,H). Furthermore, scanning electron microscopy of the surface of the endolymphatic sac/duct epithelium shows that the scattered cells with long microvilli projecting into the lumen of the normal sac/duct are not detected in the *Foxi1*$^{-/-}$ mutants (Fig. 13). This is a cell configuration that fits well with the scattered pattern of in situ hybridization signals for *Foxi1*, *Pds*, *Coch* and *Jag1* (Fig. 12). To confirm viability and biological functionality of the endolymphatic duct/sac epithelium we showed that antisera directed against E-cadherin and ZO-1 (zonula occludens), markers for biological active epithelium (Stevenson et al., 1986; Torres et al., 1996), stain wild-type and *Foxi1*$^{-/-}$ endolymphatic duct/sac epithelium equally well (not shown).

DISCUSSION

Early (E9.5-13.5) morphogenesis and patterning of the inner ear appear to proceed normally in mice lacking *Foxi1* (Figs 1, 2). Expression patterns of marker genes, known to be involved in patterning of the otic vesicle [e.g. *Eya1* (Xu et al., 1999)], vestibular development [e.g. *Otx1*, *Hmx3* (Acampora et al., 1996; Hadrys et al., 1998; Wang et al., 1998)], cochlear maturation [e.g. *Pax2* (Favor et al., 1996; Torres et al., 1996)] and a marker for neural crest cell contribution to the developing inner ear [*ErbB3* (Britsch et al., 1998; Lemke, 1996)], show no aberration in *Foxi1*$^{-/-}$ mutants. Although it is possible that some aspects of early inner ear morphogenesis, not identified by the methods used here, are affected – the otic vesicle-restricted expression of *Foxi1* at E9.5 (Hulander et al., 1998) seems to be redundant for early development of the inner ear. At later stages (E16.5) of inner ear maturation *Foxi1* expression becomes restricted to the endolymphatic duct/sac epithelium

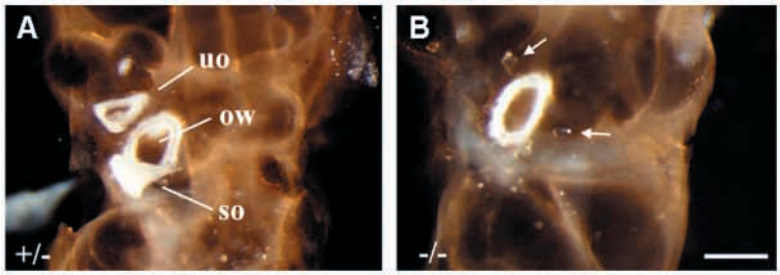

Fig. 8. Morphology of the otoconia, at E16.5, in *Foxi1*$^{+/-}$ (A) and *Foxi1*$^{-/-}$ (B) inner ears. The white utricular (uo) and saccular (so) otoconia are not formed properly (arrows) in *Foxi1*$^{-/-}$ mice (B). This finding suggests a defect in proper crystallization of calcium carbonate crystals normally found in the otoconia. In this mouse strain (CD-1), the perimeter of the oval window (ow) has a white color. Scale bar: 250 μm.

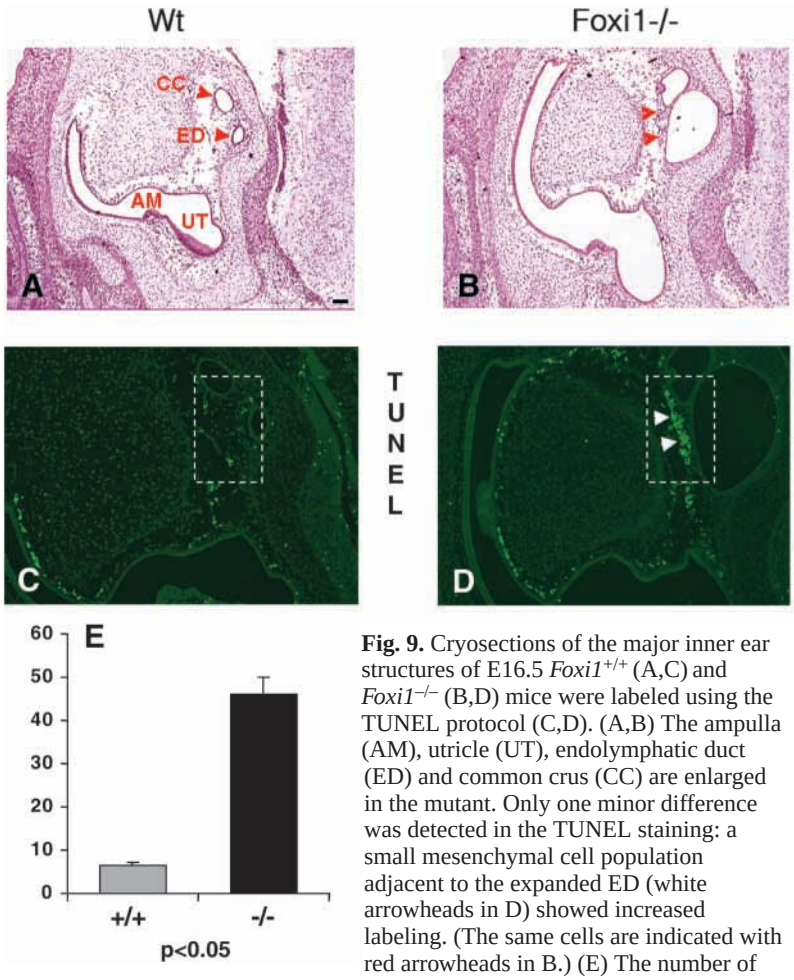

Fig. 9. Cryosections of the major inner ear structures of E16.5 *Foxi1*$^{+/+}$ (A,C) and *Foxi1*$^{-/-}$ (B,D) mice were labeled using the TUNEL protocol (C,D). (A,B) The ampulla (AM), utricle (UT), endolymphatic duct (ED) and common crus (CC) are enlarged in the mutant. Only one minor difference was detected in the TUNEL staining: a small mesenchymal cell population adjacent to the expanded ED (white arrowheads in D) showed increased labeling. (The same cells are indicated with red arrowheads in B.) (E) The number of TUNEL-positive cells were counted in anatomically corresponding sites in 5 *Foxi1*$^{+/+}$ and 5 *Foxi1*$^{-/-}$ inner ears (represented by the the boxed area in C and D). Numbers expressed as means ±s.d. Scale bar: 100 μm.

(Fig. 12A), thus delimiting this cell population as a unique pool of *Foxi1*-positive cells in contrast to the remaining otic epithelium. This epithelium is also characterized by a scattered expression of *Pds* (Fig. 12A), *Coch* (Fig. 12D) and *Jag1 (Jagged1*; Fig. 12G). The sites of wild-type *Coch* expression, in the cell layers beneath the otic epithelium in the cochlea and vestibulum reinforces the unique properties of the endolymphatic duct/sac epithelium, where *Coch* is expressed instead in the epithelial cells (Fig. 12D-F). While the fate and function of the different cell populations within this epithelium remain unclear, the punctate expression pattern of *Foxi1*, *Jag1* (Morrison et al., 1999) *Coch* and *Pds* might delimit a subset of endolymphatic duct/sac epithelium cells that could serve a common function in the mature epithelium such as resorption of endolymph. Detailed morphological analysis of the endolymphatic duct/sac epithelium, using electron microscopy, suggests the presence of at least three distinct cell types. One of these cell types project microvilli into the endolymphatic duct/sac lumen (Barbara et al., 1988b). Even though our expression data do not allow any conclusions to be made with regard to which cell type(s) express *Foxi1*, *Jag1*, *Coch* and *Pds* (Fig. 12), our experiments do provide evidence for the presence of several distinct cell types within this epithelium. The lack of cells with long microvilli projecting into the lumen of the endolymphatic sac in the *Foxi1* mutants suggests that this cell type may also express *Foxi1*, *Pds*, *Coch* and *Jag1* (Figs 12, 13). Thus, it is possible that early *Foxi1* expression, at E9.5-13.5, is important for correct patterning of endolymphatic duct/sac epithelium. We would like to speculate that this process could involve Jag1/Notch interactions and that *Foxi1* expression is needed for proper execution of such signals.

In mice that lack *Foxi1* expression, an expansion of the endolymphatic chamber becomes evident at E16.5 with the endolymphatic duct/sac as the most expanded structure (Figs 4-6). The absence of *Pds* gene expression in the epithelium of this structure (Fig. 12B) establishes *Foxi1* as an upstream regulator of *Pds* gene expression at this location. There are two possible reasons for the lack of *Pds* expression in the endolymphatic duct/sac: *Foxi1* may in a direct way regulate *Pds* expression, or without *Foxi1*, cells that normally express *Pds* may be missing. *Pds* gene expression in the cochlea and vestibulum is unaffected by the lack of *Foxi1*, suggesting that expression at these locations is regulated by other factors. Both *Coch* and *Jag1* expression are also dependent on *Foxi1* in the endolymphatic duct/sac while expression at other sites in the developing inner ear is not (Fig. 12D-H). In the inner ear of wild-type mice, *Pds* gene expression is first visualized in the prospective endolymphatic duct/sac epithelium at approximately E13. Two days later at

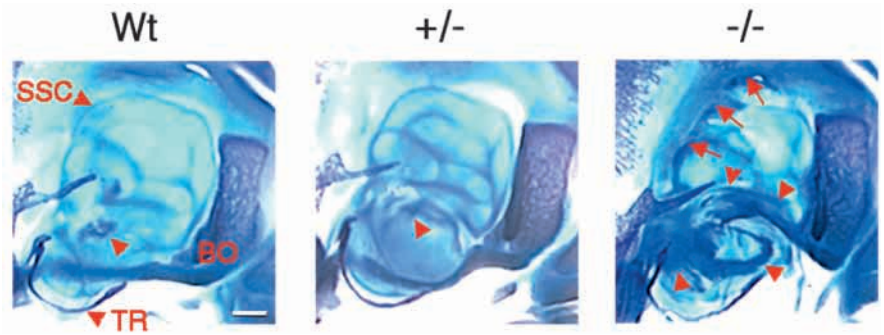

Fig. 10. Heads stained for bone (dark purple) and cartilage (blue) at E18.5. Superior semicircular canal (SSC), tympanic ring (TR) and the basioccipital bone (BO) are marked. In *Foxi1*$^{+/+}$ and *Foxi1*$^{+/-}$ an arrowhead indicates the ossification centers of the middle ear bones. Normal morphology is seen in *Foxi1*$^{+/+}$ and *Foxi1*$^{+/-}$ mice; *Foxi1*$^{-/-}$ animals display a clearly aberrant integration of the otic capsule in the temporal bone as evident by excessive ectopic cartilage condensation/bone formation in both the cochlea (arrowheads) and the vestibulum (arrows). Scale bar: 200 μm.

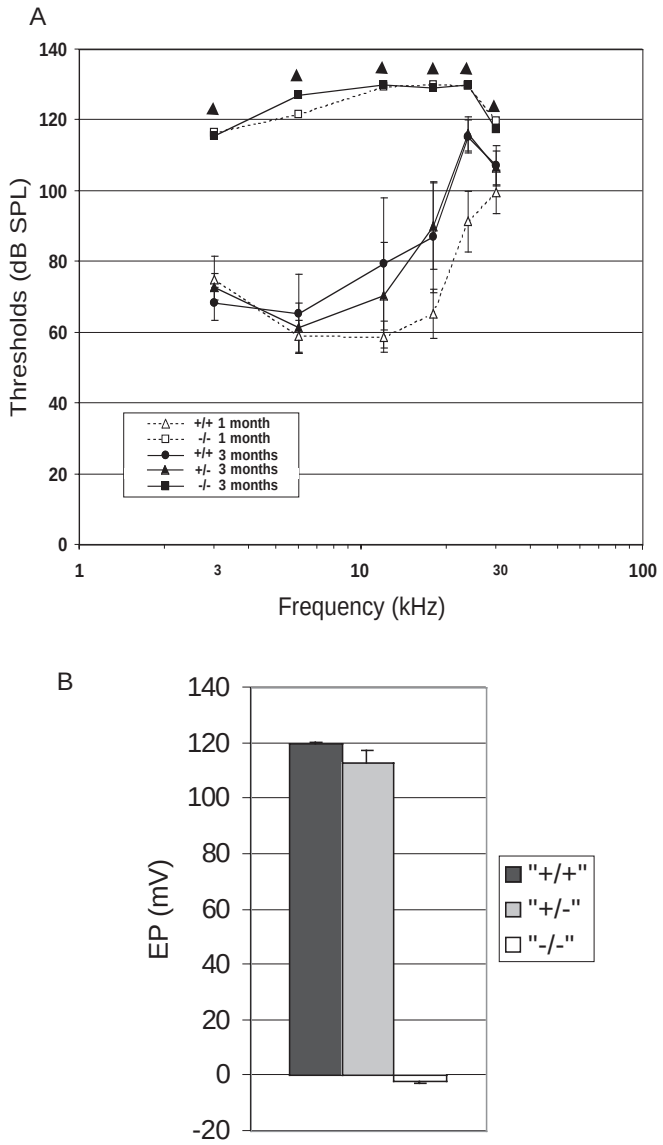

Fig. 11. (A) A compound action potential response, measured from the round window of the cochlea. *Foxi1*$^{+/+}$and *Foxi1*$^{+/-}$ littermates showed thresholds (±s.e.m.) that were very similar to each other, but relatively high compared with other mouse strains especially at high frequencies, suggesting that the genetic background of these mice (mostly CD-1) was associated with poor hearing. *Foxi1*$^{-/-}$ mice showed no cochlear responses of any sort, up to maximum sound output used; indicated by the black triangles at the top of the graph (*n*=7, *Foxi1*$^{+/+}$; *n*=9, *Foxi1*$^{+/-}$; *n*=10, *Foxi1*$^{-/-}$). (B) Mean endocochlear potentials (EP; ±s.e.m.) from wild type, heterozygote and null mutant littermates aged 29 to 129 days. There was no difference in the EPs in wild types and heterozygotes, but homozygous mutants showed potentials close to zero (*n*=14, *Foxi1*$^{+/+}$; *n*=18, *Foxi1*$^{+/-}$; *n*=19, *Foxi1*$^{-/-}$).

E15 *Pds* gene expression is also found in the non-sensory regions adjacent to the maculae of the saccule and utricle as well as in the cells beneath the spiral prominence on the lateral wall of the external sulcus in the cochlea (Everett et al., 1999). It is interesting to note that the expansion of the endolymphatic compartment, in *Foxi1*$^{-/-}$ embryos, starts between E13.5 and E16.5 (Figs 4, 5, 6) – the same time span during which *Pds* gene expression first becomes detectable in wild-type mice (Everett et al., 1999). Taken together these findings support the idea that the inner ear phenotype in *Foxi1*$^{-/-}$ mice is, at least to some extent, due to lack of pendrin expression in the endolymphatic duct/sac epithelium. This hypothesis is further supported by the fact that patients with Pendred syndrome display enlargement of the endolymphatic duct and sac as a constant feature (Phelps et al., 1998). As a consequence of this, it seems that *Pds* gene expression at inner ear locations other than the endolymphatic duct/sac epithelium is not sufficient to substitute for the lack of *Pds* expression in the endolymphatic duct/sac epithelium and hinder the abnormal expansion of the endolymphatic compartment. Alternatively, the expression at these locations, initiated at E15, is not capable of reversing the presumably established state of dysfunction in the endolymphatic duct/sac epithelium, involving not only *Pds* gene expression but also *Coch* and *Jag1*. The exact order of events underlying the phenotype described here is not resolved. It is however possible that Notch-mediated patterning of the endolymphatic epithelium, supported by early (E9.5) *Foxi1* expression, is disturbed because of a lack of *Jag1* and that this leads to lack of a specialized cell type that expresses pendrin and serves as a major site for endolymph resorption (Fig. 13). Alternatively, it is also conceivable that lack of pendrin expression leads to a state of epithelial dysfunction not compatible with *Jag1* and *Coch* expression, at a later stage of inner ear development. Such dysfunction could not be too pronounced since expression of both E-cadherin and ZO-1, markers of biologically active epithelium, are unaffected by the absence of *Foxi1* expression (not shown). Nevertheless a gene regulatory hierarchy has been established in which *Foxi1* is upstream of *Pds*, *Coch* and *Jag1*. Further support for our suggestion that abnormal *Pds* expression may underlie the pathology we observe in *Foxi1* mutants comes from the *Pds* mutant mouse, which shows a similar early expansion of the endolymphatic compartments including endolymphatic duct and sac and resultant malformation (Everett et al., 2001).

Only minor differences in TUNEL (Fig. 9) and BrdU (not shown) labeling can be demonstrated. The abnormalities revealed by bone and cartilage staining (Fig. 10) are interesting since epithelial-mesenchymal interactions are necessary for condensation of the periotic-mesenchyme during formation of the otic capsule (Frenz and Van De Water, 1991; Van de Water and Ruben, 1971). Results from bone and cartilage staining demonstrate an altered gross morphology of the otic capsule in *Foxi1* null embryos at E18.5. This may be due to increased endolymphatic pressure, leading to expansion of the endolymphatic compartment, resulting from defective pendrin-mediated chloride ion resorption. It should be noted that a defect in epithelial-mesenchymal interaction could not be ruled out as the primary defect of the abnormal otic capsule. However, it seems unlikely since *Foxi1* expression at E16.5 is restricted to the endolymphatic duct/sac epithelium, which is located outside the otic capsule. One consequence of altered function of the endolymphatic duct/sac epithelium is most likely a change in ionic composition of the endolymph as demonstrated by lack of proper crystallization of the otoconia (Fig. 8). The complete hearing loss together with an endocochlear potential (EP) of approximately 0 mV in *Foxi1* null mutants (Fig. 11A,B) suggest a severe ‘ion channelopathy’ possibly in combination with a rupture of the endolymphatic

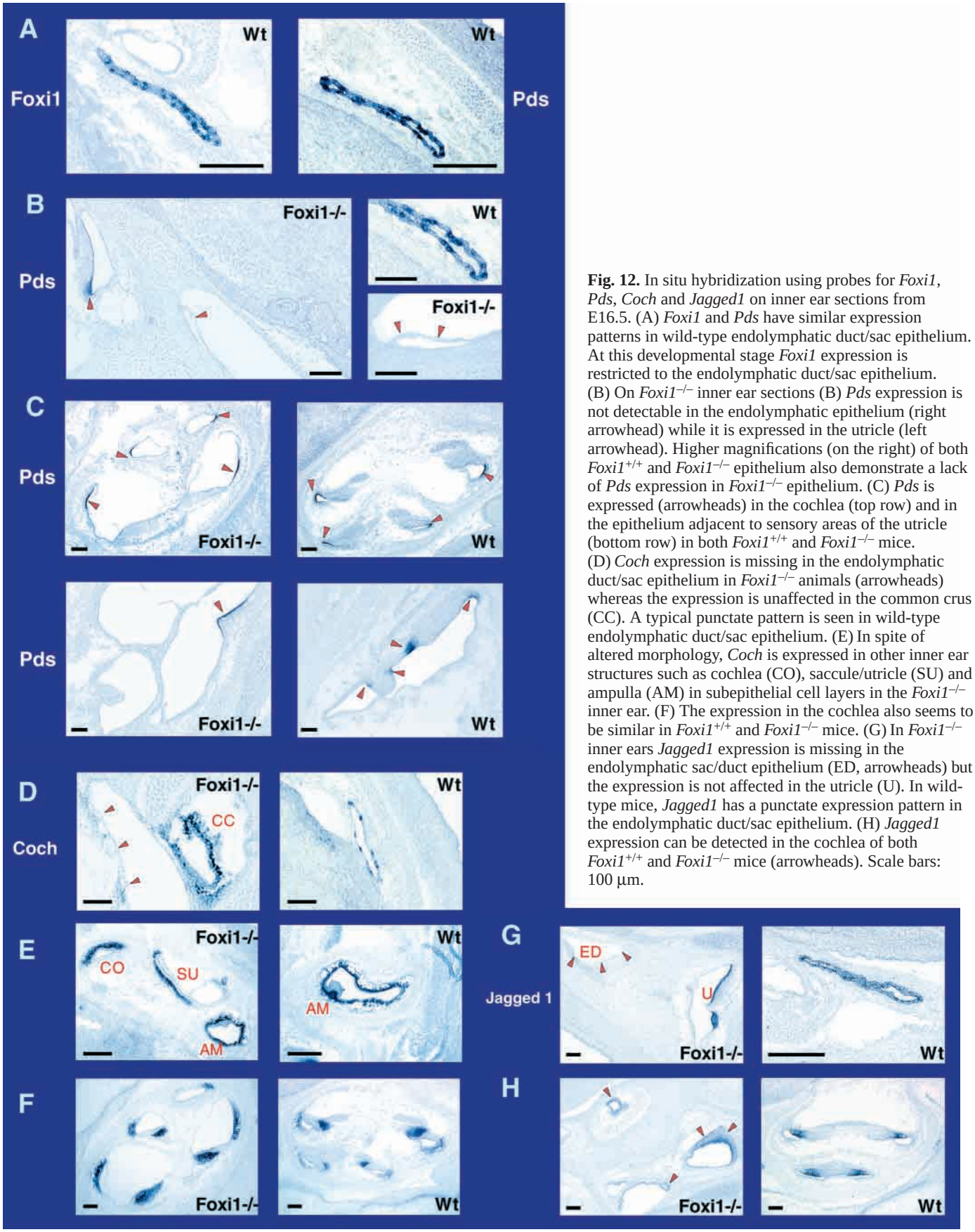

Fig. 12. In situ hybridization using probes for *Foxi1*, *Pds*, *Coch* and *Jagged1* on inner ear sections from E16.5. (A) *Foxi1* and *Pds* have similar expression patterns in wild-type endolymphatic duct/sac epithelium. At this developmental stage *Foxi1* expression is restricted to the endolymphatic duct/sac epithelium. (B) On *Foxi1*$^{-/-}$ inner ear sections (B) *Pds* expression is not detectable in the endolymphatic epithelium (right arrowhead) while it is expressed in the utricle (left arrowhead). Higher magnifications (on the right) of both *Foxi1*$^{+/+}$ and *Foxi1*$^{-/-}$ epithelium also demonstrate a lack of *Pds* expression in *Foxi1*$^{-/-}$ epithelium. (C) *Pds* is expressed (arrowheads) in the cochlea (top row) and in the epithelium adjacent to sensory areas of the utricle (bottom row) in both *Foxi1*$^{+/+}$ and *Foxi1*$^{-/-}$ mice. (D) *Coch* expression is missing in the endolymphatic duct/sac epithelium in *Foxi1*$^{-/-}$ animals (arrowheads) whereas the expression is unaffected in the common crus (CC). A typical punctate pattern is seen in wild-type endolymphatic duct/sac epithelium. (E) In spite of altered morphology, *Coch* is expressed in other inner ear structures such as cochlea (CO), saccule/utricle (SU) and ampulla (AM) in subepithelial cell layers in the *Foxi1*$^{-/-}$ inner ear. (F) The expression in the cochlea also seems to be similar in *Foxi1*$^{+/+}$ and *Foxi1*$^{-/-}$ mice. (G) In *Foxi1*$^{-/-}$ inner ears *Jagged1* expression is missing in the endolymphatic sac/duct epithelium (ED, arrowheads) but the expression is not affected in the utricle (U). In wild-type mice, *Jagged1* has a punctate expression pattern in the endolymphatic duct/sac epithelium. (H) *Jagged1* expression can be detected in the cochlea of both *Foxi1*$^{+/+}$ and *Foxi1*$^{-/-}$ mice (arrowheads). Scale bars: 100 μm.

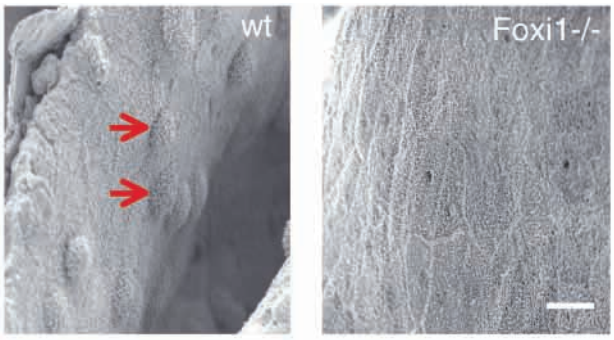

Fig. 13. Scanning electron micrographs of endolymphatic duct/sac epithelium (E14.5) from *Foxi1*$^{+/+}$ and *Foxi1*$^{-/-}$ mice. Arrows (in wild type) indicate two cells of a type we call forkhead related (FORE) cells, that are missing in *Foxi1*$^{-/-}$ epithelium. Scale bar: 10 μm.

epithelium allowing peri- and endolymph, to mix. However, we cannot decisively determine which of these two factors is the major cause of deafness. We would like to speculate that the findings of (i) a progressive thinning of the endolymphatic epithelium (Figs 4, 7), (ii) lack of a perilymphatic compartment in the cochlea (Fig. 7D), (iii) expansion of endolymphatic compartments in the vestibulum (Fig. 7C) and (iv) an EP of 0 mV (Fig. 11B) all are compatible with a more or less total rupture of the endolymphatic epithelium. Nevertheless, it is most likely that the initial event is an expansion of the endolymphatic compartment due to a defective ionic composition, possibly including an increased osmolarity of the endolymph, which in turn severely affects the ability of stria vascularis to maintain a proper EP. A rupture of the endolymphatic epithelium at P12, as suggested by the results in Fig. 7, would further hamper this function.

The molecular mechanisms governing transformation of the near spherical otocyst into a highly complex sensory organ – the inner ear – remain to a large extent obscure. One obvious task during this process is to guide morphogenetic events that produce the intricate three-dimensional structure of the mature inner ear. In many instances during embryogenesis, formation of complex structures is achieved through preprogrammed alterations in rate of cell proliferation and/or apoptosis, e.g. limb formation. However, a recent study addressing this in the developing inner ear of chicken failed to demonstrate a clear increase in cell proliferation during outgrowth of endolymphatic duct and canal plates (Lang et al., 2000). Instead differences in the number of cells in various regions of the otic vesicle was noted, suggesting that cells were redistributed. For instance, the dorsal aspect of the otic vesicle (giving rise to the endolymphatic duct and sac) was found to undergo thinning of the epithelial surface with only a slightly increased cell proliferation (Lang et al., 2000). It is intriguing that several aspects of the inner ear phenotype seen in *Foxi1*$^{-/-}$ mice bear resemblance to that seen in *Hoxa1*$^{-/-}$and *Fgf3*$^{-/-}$ animals (Chisaka et al., 1992; Lufkin et al., 1991; Mansour et al., 1993). During early embryonic development the endolymphatic duct/sac fails to form in *Hoxa1*$^{-/-}$ and *Fgf3*$^{-/-}$ mice and the inner ear develops into large irregular cavities or has a distended and swollen appearance, respectively. This finding underscores the importance of an intact endolymphatic duct/sac, for normal inner ear development. Although there are many differences between *Foxi1*, *Hoxa1* and *Fgf3* mutants, they might all reflect the consequences of inappropriate endolymph turnover resulting from a lack of (*Hoxa1*$^{-/-}$, *Fgf3*$^{-/-}$) or inadequate function (*Foxi1*$^{-/-}$) of the endolymphatic duct/sac epithelium. The phenotypic differences could be explained by the temporal appearance of these defects, early at the otic vesicle stage in *Hoxa1* null mutants and late in the case of *Foxi1*$^{-/-}$ mice. These models also emphasize the need for tightly regulated endolymph secretion/resorption during normal inner ear development. It is possible that normal inner ear development is dependent upon ‘pressure driven’ events. This idea is supported by the finding that the initial events in outgrowth of the endolymphatic duct are not correlated with increased cell proliferation but rather thinning of the epithelial surface (Lang et al., 2000).

The endolymphatic duct and sac are crucial for maintaining proper osmotic pressure and ionic composition of the endolymph. These structures can function as an expansion chamber and expand beyond the inner ear compartment into the interdural space. In this way variations in the production of endolymph can be tolerated without any significant increase of inner ear pressure (Barbara et al., 1988a; Everett et al., 1999). This is emphasized by the fact that one experimental approach to induce inner ear hydrops is by obliteration of the endolymphatic duct/sac (Kimura and Schuknecht, 1965). The endolymphatic duct/sac epithelium is also important for absorption of endolymph (Everett et al., 1999) – several ion transporters are expressed here such as the chloride transporter pendrin (Everett et al., 1999). The relevance of this for the pathogenesis of human inner ear diseases is exemplified by conditions such as Ménière’s disease and Pendred syndrome which are both, to some extent, associated with inner ear hydrops (i.e. accumulation of endolymph in the inner ear resulting in hampered inner ear function) and an expanded endolymphatic duct/sac (Everett et al., 1999; Phelps et al., 1998; Schuknecht and Gulya, 1983). We would also like to point out that mutations in the *COCH* gene have been linked to Ménière’s disease (Fransen et al., 1999). The finding of a specific cell type, with projecting microvilli, in the endolymphatic duct/sac epithelium that most likely expresses *Foxi1*, *Pds*, *Coch* and *Jag1* raises the intriguing possibility that these FORE (**fo**rkhead **re**lated) cells (Fig. 13) are important for maintaining proper volume and/or composition of the endolymph. The FORE cell, here genetically defined, has many similarities with a morphologically identified cell type called ‘mitochondria-rich’ cell. (Qvortrup and Bretlau, 2002). We would like to speculate that the FORE cell could prove to play a role in diseases characterized by altered endolymph turnover/composition, e.g. Pendred syndrome and Ménière’s disease.

FOXI1 (also known as *FKHL10*), the human homologue of *Foxi1*, has been mapped to the chromosomal localization of 5q32-34 (Larsson et al., 1995). To this date no human disease has been linked to mutations in this gene. As much as 10% of all hereditary deafness could be due to Pendred syndrome (Fraser, 1965) and as many as 23% of the patients with a clinical diagnosis of Pendred syndrome lack mutations in the *PDS* gene (Reardon et al., 2000). This implies that mutations in *FOXI1* could prove to be a cause of human deafness.

We thank Karen B. Avraham, Guy Van Camp, Claes Möller and William Reardon for valuable discussions, C. Birchmeier, E. Green, P. Gruss, C. Hodgetts, T. Lufkin, A. Matthews and C. Morton for sharing probes with us, H. Semb for making antisera available and Tim Folkard for help with setting up the three-dimensional reconstruction system. This work was made possible with support from the UK MRC and EC contract CT97-2715, The Swedish Medical Research Foundation, The Arne and IngaBritt Lundberg Foundation, The Juvenile Diabetes Foundation, The Wallenberg Foundation, The Swedish Foundation for Strategic Research (Nucleic Acid Program), a Junior Individual Grant from The Swedish Foundation for Strategic Research to S.E., an EMBO short term fellowship to M.H.

REFERENCES

Acampora, D., Mazan, S., Avantaggiato, V., Barone, P., Tuorto, F., Lallemand, Y., Brulet, P. and Simeone, A. (1996). Epilepsy and brain abnormalities in mice lacking the Otx1 gene. *Nat. Genet.* **14**, 218-222.

Barbara, M., Rask-Andersen, H. and Bagger-Sjoback, D. (1988a). Morphology of the endolymphatic duct and sac in the Mongolian gerbil. *Acta Otolaryngol.* **105**, 31-38.

Barbara, M., Rask-Andersen, H. and Bagger-Sjoback, D. (1988b). The surface morphology of the endolymphatic sac of the Mongolian gerbil (Meriones unguiculatus) (a scanning electron microscopic study). *J. Laryngol. Otol.* **102**, 308-313.

Bostrom, H., Willetts, K., Pekny, M., Leveen, P., Lindahl, P., Hedstrand, H., Pekna, M., Hellstrom, M., Gebre-Medhin, S., Schalling, M. et al. (1996). PDGF-A signaling is a critical event in lung alveolar myofibroblast development and alveogenesis. *Cell* **85**, 863-873.

Britsch, S., Li, L., Kirchhoff, S., Theuring, F., Brinkmann, V., Birchmeier, C. and Riethmacher, D. (1998). The ErbB2 and ErbB3 receptors and their ligand, neuregulin-1, are essential for development of the sympathetic nervous system. *Genes Dev.* **12**, 1825-1836.

Chisaka, O., Musci, T. S. and Capecchi, M. R. (1992). Developmental defects of the ear, cranial nerves and hindbrain resulting from targeted disruption of the mouse homeobox gene Hox-1.6. *Nature* **355**, 516-520.

Corey, D. P. and Hudspeth, A. J. (1983). Analysis of the microphonic potential of the bullfrog's sacculus. *J. Neurosci.* **3**, 942-961.

Davis, A. C. (1995). *Hearing in Adults*. London: Whurr.

Delpire, E., Lu, J., England, R., Dull, C. and Thorne, T. (1999). Deafness and imbalance associated with inactivation of the secretory Na- K-2Cl co-transporter. *Nat. Genet.* **22**, 192-195.

Dixon, M. J., Gazzard, J., Chaudhry, S. S., Sampson, N., Schulte, B. A. and Steel, K. P. (1999). Mutation of the Na-K-Cl co-transporter gene Slc12a2 results in deafness in mice. *Hum. Mol. Genet.* **8**, 1579-1584.

Everett, L. A., Glaser, B., Beck, J. C., Idol, J. R., Buchs, A., Heyman, M., Adawi, F., Hazani, E., Nassir, E., Baxevanis, A. D. et al. (1997). Pendred syndrome is caused by mutations in a putative sulphate transporter gene (PDS). *Nat. Genet.* **17**, 411-422.

Everett, L. A., Morsli, H., Wu, D. K. and Green, E. D. (1999). Expression pattern of the mouse ortholog of the Pendred's syndrome gene (Pds) suggests a key role for pendrin in the inner ear. *Proc. Natl. Acad. Sci. USA* **96**, 9727-9732.

Everett, L. A., Belyantseva, I. A., Noben-Trauth, K., Cantos, R., Chen, A., Thakkar, S. I., Hoogstraten-Miller, S. H., Kachar, B., Wu, D. K. and Green, E. P. (2001). Targeted disruption of mouse *Pds* provides insight about the inner-ear defects encountered in Pendred syndrome. *Hum. Mol. Genet.* **10**, 153-161.

Favor, J., Sandulache, R., Neuhauser-Klaus, A., Pretsch, W., Chatterjee, B., Senft, E., Wurst, W., Blanquet, V., Grimes, P., Sporle, R. and Schughart, K. (1996). The mouse Pax2 (1Neu) mutation is identical to a human PAX2 mutation in a family with renal-coloboma syndrome and results in developmental defects of the brain, ear, eye, and kidney. *Proc. Natl. Acad. Sci.* **93**, 13870-13875.

Fortnum, H. M., Summerfield, A. Q., Marshall, D. H., Davis, A. C. and Bamford, J. M. (2001). Prevalence of permanent childhood hearing impairment in the United Kingdom and implications for universal neonatal hearing screening: questionnaire based ascertainment study. *Brit. Med. J.* **323**, 1-6.

Fransen, E., Verstreken, M., Verhagen, W. I., Wuyts, F. L., Huygen, P. L., D'Haese, P., Robertson, N. G., Morton, C. C., McGuirt, W. T., Smith, R. J. et al. (1999). High prevalence of symptoms of Meniere's disease in three families with a mutation in the COCH gene. *Hum. Mol. Genet.* **8**, 1425-1429.

Fraser, G. R. (1965). Association of congenital deafness with goitre (Pendred's syndrome): a study of 207 families. *Ann. Hum. Genet.* **28**, 201-249.

Frenz, D. A. and van de Water, T. R. (1991). Epithelial control of periotic mesenchyme chondrogenesis. *Dev. Biol.* **144**, 38-46.

Hadrys, T., Braun, T., Rinkwitz-Brandt, S., Arnold, H. H. and Bober, E. (1998). Nkx5-1 controls semicircular canal formation in the mouse inner ear. *Development* **125**, 33-39.

Howard, J. and Hudspeth, A. J. (1988). Compliance of the hair bundle associated with gating of mechanoelectrical transduction channels in the bullfrog's saccular hair cell. *Neuron* **1**, 189-199.

Hulander, M., Wurst, W., Carlsson, P. and Enerback, S. (1998). The winged helix transcription factor Fkh10 is required for normal development of the inner ear. *Nat. Genet.* **20**, 374-376.

Hutson, M. R., Lewis, J. E., Nguyen-Luu, D., Lindberg, K. H. and Barald, K. F. (1999). Expression of pax2 and patterning of the chick inner ear. *J. Neurocytol.* **28**, 795-807.

Johnsen, T., Jorgensen, M. B. and Johnsen, S. (1986). Mondini cochlea in Pendred's syndrome. A histological study. *Acta Otolaryngol.* **102**, 239-247.

Karet, F. E., Finberg, K. E., Nelson, R. D., Nayir, A., Mocan, H., Sanjad, S. A., Rodriguez-Soriano, J., Santos, F., Cremers, C. W., di Pietro, A. et al. (1999). Mutations in the gene encoding B1 subunit of H+-ATPase cause renal tubular acidosis with sensorineural deafness. *Nat. Genet.* **21**, 84-90.

Kimura, R. S. and Schuknecht, H. F. (1965). Membraneous hydrops in the inner ear of the guinea pig after obliteration of the endolymphatic sac. *Pract. Oto-Rhino-Laryngol.* **27**, 343-354.

Kubisch, C., Schroeder, B. C., Friedrich, T., Lutjohann, B., El-Amraoui, A., Marlin, S., Petit, C. and Jentsch, T. J. (1999). KCNQ4, a novel potassium channel expressed in sensory outer hair cells, is mutated in dominant deafness. *Cell* **96**, 437-446.

Lang, H., Bever, M. M. and Fekete, D. M. (2000). Cell proliferation and cell death in the developing chick inner ear: spatial and temporal patterns. *J. Comp. Neurol.* **417**, 205-220.

Larsson, C., Hellqvist, M., Pierrou, S., White, I., Enerback, S. and Carlsson, P. (1995). Chromosomal localization of six human forkhead genes, freac-1 (FKHL5), -3 (FKHL7), -4 (FKHL8), -5 (FKHL9), -6 (FKHL10), and -8 (FKHL12). *Genomics* **30**, 464-469.

Lawoko-Kerali, G., Rivolta, N. K. and Holley, M. (2002). Expression of the transcription factors GATA3 and Pax2 during development of the mammalian inner ear. *J. Comp. Neurol.* **442**, 378-391.

Lemke, G. (1996). Neuregulins in development. *Mol. Cell. Neurosci.* **7**, 247-262.

Li, X. C., Everett, L. A., Lalwani, A. K., Desmukh, D., Friedman, T. B., Green, E. D. and Wilcox, E. R. (1998). A mutation in PDS causes non-syndromic recessive deafness. *Nat. Genet.* **18**, 215-217.

Lufkin, T., Dierich, A., LeMeur, M., Mark, M. and Chambon, P. (1991). Disruption of the Hox-1.6 homeobox gene results in defects in a region corresponding to its rostral domain of expression. *Cell* **66**, 1105-1119.

Mansour, S. L., Goddard, J. M. and Capecchi, M. R. (1993). Mice homozygous for a targeted disruption of the proto-oncogene int-2 have developmental defects in the tail and inner ear. *Development* **117**, 13-28.

Martin, P. and Swanson, G. J. (1993). Descriptive and experimental analysis of the epithelial remodellings that control semicircular canal formation in the developing mouse inner ear. *Dev. Biol.* **159**, 549-558.

McLeod, M. J. (1980). Differential staining of cartilage and bone in whole mouse fetuses by alcian blue and alizarin red S. *Teratology* **22**, 299-301.

Mondini, C. (1791). Anatomica surdi natisectio: De Bononiensi Scientarium et artium Instituto atque academia commentarii. *Bononia VII (Opuscula)*, 419-428.

Morrison, A., Hodgetts, C., Gossler, A., Hrabe de Angelis, M. and Lewis, J. (1999). Expression of Delta1 and Serrate1 (Jagged1) in the mouse inner ear. *Mech. Dev.* **84**, 169-172.

Morsli, H., Tuorto, F., Choo, D., Postiglione, M. P., Simeone, A. and Wu, D. K. (1999). Otx1 and Otx2 activities are required for the normal development of the mouse inner ear. *Development* **126**, 2335-2343.

Neyroud, N., Tesson, F., Denjoy, I., Leibovici, M., Donger, C., Barhanin, J., Faure, S., Gary, F., Coumel, P., Petit, C. et al. (1997). A novel mutation in the potassium channel gene KVLQT1 causes the Jervell and Lange-Nielsen cardioauditory syndrome. *Nat. Genet.* **15**, 186-189.

Phelps, P. D., Coffey, R. A., Trembath, R. C., Luxton, L. M., Grossman, A. B., Britton, K. E., Kendall-Taylor, P. Graham, J. M., Cadge, B. C., Stephens, S. G., et al. (1998). Radiological malformations of the ear in Pendred syndrome. *Clin. Radiol.* **53**, 268-273.

Qvortrup, K. and Bretlau, P. (2002). The endolymphatic sac: A scanning and transmission electron microscopy study. *ORL* **64**, 129-137.

Reardon, W., O'Mahoney, C., Trembath, R., Jan, H. and Phelps, P. D. (2000). Enlarged vestibular aqueduct: a radiological marker of pendred syndrome, and mutation of the PDS gene. *Q. J. Med.* **93**, 99-104.

Robertson, N. G., Lu, L., Heller, S., Merchant, S. N., Eavey, R. D., McKenna, M., Nadol, J. B., Jr, Miyamoto, R. T., Linthicum, F. H., Jr, Lubianca Neto, J. F. et al. (1998). Mutations in a novel cochlear gene cause DFNA9, a human nonsyndromic deafness with vestibular dysfunction. *Nat. Genet.* **20**, 299-303.

Robertson, N. G., Skvorak, A. B., Yin, Y., Weremowicz, S., Johnson, K. R., Kovatch, K. A., Battey, J. F., Bieber, F. R. and Morton, C. C. (1997). Mapping and characterization of a novel cochlear gene in human and in mouse: a positional candidate gene for a deafness disorder. DFNA9. *Genomics* **46**, 345-354.

Rosen, B. and Beddington, R. S. (1993). Whole-mount in situ hybridization in the mouse embryo: gene expression in three dimensions. *Trends Genet.* **9**, 162-167.

Sahly, I., Andermann, P. and Petit, C. (1999). The zebrafish eya1 gene and its expression pattern during embryogenesis. *Dev. Genes Evol.* **209**, 399-410.

Schuknecht, H. F. and Gulya, A. J. (1983). Endolymphatic hydrops. An overview and classification. *Ann. Otol. Rhinol. Laryngol.* Suppl. **106**, 1-20.

Shone, G., Raphael, Y. and Miller, J. M. (1991). Hereditary deafness occurring in cd/1 mice. *Hear. Res.* **57**, 153-156.

Steel, K. P. (1999). Perspectives: biomedicine. The benefits of recycling. *Science* **285**, 1363-1364.

Steel, K. P. and Bussoli, T. J. (1999). Deafness genes: expressions of surprise. *Trends Genet.* **15**, 207-211.

Steel, K. P. and Smith, R. J. (1992). Normal hearing in Splotch (Sp/+), the mouse homologue of Waardenburg syndrome type 1. *Nat. Genet.* **2**, 75-79.

Stevenson, B. R., Siliciano, J. D., Mooseker, M. S. and Goodenough, D. A., Phelps, P. D., Coffey, R. A., Trembath, R. C., Luxon, L. M., Grossman, A. B., Britton, K. E., Kendall-Taylor, P., Graham, J. M., Cadge, B. C., Stephens, S. G. et al. (1986). Identification of ZO-1: a high molecular weight polypeptide associated with the tight junction (zonula occludens) in a variety of epithelia. *J. Cell Biol.* **103**, 755-766.

Torres, M., Gomez-Pardo, E. and Gruss, P. (1996). Pax2 contributes to inner ear patterning and optic nerve trajectory. *Development* **122**, 3381-3391.

Van de Water, T. R. and Ruben, R. J. (1971). Organ culture of the mammalian inner ear. *Acta Otolaryngol.* **71**, 303-312.

Vetter, D. E., Mann, J. R., Wangemann, P., Liu, J., McLaughlin, K. J., Lesage, F., Marcus, D. C., Lazdunski, M., Heinemann, S. F. and Barhanin, J. (1996). Inner ear defects induced by null mutation of the isk gene. *Neuron* **17**, 1251-1264.

Wang, W., van de Water, T. and Lufkin, T. (1998). Inner ear and maternal reproductive defects in mice lacking the Hmx3 homeobox gene. *Development* **125**, 621-634.

Wilson, J. (1985). Deafness in developing countries. Approaches to a global program of prevention. *Arch. Otolaryngol.* **111**, 2-9.

Wu, D. K. and Oh, S. H. (1996). Sensory organ generation in the chick inner ear. *J. Neurosci.* **16**, 6454-6462.

Xu, P. X., Adams, J., Peters, H., Brown, M. C., Heaney, S. and Maas, R. (1999). Eya1-deficient mice lack ears and kidneys and show abnormal apoptosis of organ primordia. *Nat. Genet.* **23**, 113-117.

Zheng, J., Shen, W., He, D. Z., Long, K. B., Madison, L. D. and Dallos, P. (2000). Prestin is the motor protein of cochlear outer hair cells. *Nature* **405**, 149-155.